

Multipartite purification protocols: upper and optimal bounds

Alastair Kay and Jiannis K. Pachos

*Centre for Quantum Computation, Department of Applied Mathematics and Theoretical Physics,
University of Cambridge, Cambridge CB3 0WA, UK*

(Dated: August 3, 2018)

A method for producing an upper bound for all multipartite purification protocols is devised, based on knowing the optimal protocol for purifying bipartite states. When applied to a range of noise models, both local and correlated, the optimality of certain protocols can be demonstrated for a variety of graph and valence bond states.

I. INTRODUCTION

Quantum states of many qubits are essential ingredients in the functioning of quantum computers, and yet their properties, such as entanglement, are poorly understood. Of particular interest are graph states, which provide a range of benefits for communication and cryptography [1]. In addition, they form a universal resource for quantum computation [2, 3] and enable computation in scenarios where the employed two-qubit gate is probabilistic [4, 5, 6]. However, any practical implementation will introduce noise to the system. The noise-induced errors need to be minimized, and corrected, before a practical application of these states is considered. One way to achieve this is by purification, where many copies of the noisy state are combined to yield a single perfect copy.

The concentration of entanglement in two-qubit systems has yielded some important results in quantum information, such as secure communication via privacy amplification [7]. Nevertheless, the detailed study of similar transformations in many-qubit systems has only recently commenced. The purification of two-qubit states was first examined in [7, 8], and the performance of these protocols is optimal if the operations are perfect. The efficacy of the proposed protocols in the presence of noise was explored in [9]. Subsequently, the question of purifying multipartite states has arisen [10]. A variety of protocols have been discussed, starting from a subset of graph states [11, 12] and generalizing to arbitrary graph [13] and stabilizer states [14]. These different protocols tend to trade between a large tolerance of noise [11, 12] and the scaling of purification rate [15]. To date, little has been said on the subject of what is optimal, although some (non-tight) bounds have previously been found, such as in the case of independent local Z -noise [16], or for GHZ states [17, 18, 19].

In this paper, we prove the optimality of certain purification protocols for a variety of noise models by considering general upper bounds. These derivations are based on a central theorem that analyzes the purification of multipartite states in terms of the purification of bipartite states, and hence allows for a direct extension of previous optimality proofs. When restricted to Z -noise, the application of the theorem becomes straightforward for a certain class of graph states called locally reconstructible states. These states allow for the direct application of

the optimal bipartite purification protocol for each link of the graph, thus extending it to the multipartite case. Subsequently, a wide range of upper bounds in the tolerated error rates are derived for a variety of error models and states, while optimality is numerically demonstrated in certain cases.

The paper is organized as follows. After an initial introduction to graph states (Sec. II) and purification protocols (Sec. III), we introduce our main theorem in Sec. III C, which proves that if purification of a bipartite state is impossible, so is the purification of related multipartite states. This result is applied to a variety of error models in Sec. IV, including local Z -noise and depolarizing noise. For the case of Z -noise we prove optimality of the two purification protocols under consideration for a sub-class of graph states. In the case of maximally depolarizing noise, we prove a universal bound which applies to all graph states. Finally, in Sec. V, we derive an example of a valence bond state that can be optimally purified, proving that our method is not merely limited to graph states. Critically, the example that we produce has a finite entanglement length. The presented results expand and extend the work of [20].

II. GRAPH STATES

For the majority of this paper, we will be interested in the purification of graph states. These can be defined in two equivalent ways. With a particular graph G , we can associate a set of vertices, V_G , and edges, E_G , which connect pairs of vertices. The first way to define a pure graph state is as the ground state of the Hamiltonian

$$H = \sum_{i \in V_G} J_i X_i \prod_{\{i,j\} \in E_G} Z_j, \quad (1)$$

where we have attached a qubit to each vertex and X_i and Z_j are the familiar Pauli matrices applied to qubits i and j respectively. The individual terms $K_i = X_i \prod_{\{i,j\} \in E_G} Z_j$ commute with each other, $[K_i, K_j] = 0$, and thus stabilize the graph state. These are scaled by arbitrary coupling strengths J_i , which we will subsequently take to be equal. We note that $[K_i, Z_j] = 0$ if $i \neq j$, and $\{K_i, Z_i\} = 0$, which means that the excited states of the Hamiltonian are described by local Z -rotations, and that these local rotations constitute a complete, orthogonal

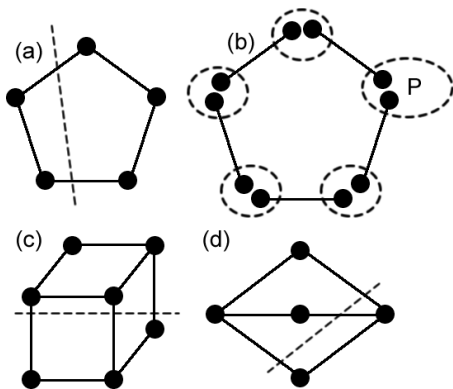


FIG. 1: (a) A pentagon is locally reconstructible, but not two-colorable. This graph is locally equivalent to the five-qubit error correcting code. (b) The pentagon can be formed from two-qubit pairs by applying the projector $P = |0\rangle\langle 00| + |1\rangle\langle 11|$ to each pair of qubits that needs to be combined. (c) The graph state which is locally equivalent to the codewords of the Steane-[[7,1,3]] error correcting code. (d) A shape which is two-colorable, but not locally reconstructible.

basis over the Hilbert space associated with the graph. An equivalent way to define a graph state is in a more operational sense, where we prepare each qubit in the state $|+\rangle = (|0\rangle + |1\rangle)/\sqrt{2}$, and apply controlled-phase gates along each edge of the graph.

For what follows, the action of measurements on a graph state are of particular interest [21]. A Z -measurement removes a vertex from the graph, along with its edges. If we wish to form a graph state from two-qubit states corresponding to the edges of the graph, it is simplest to revert to the matrix product state formalism [22], where we apply measurements on all of the qubits that need to be combined to a single qubit. In the case of a linear cluster state, this simply corresponds to performing a controlled-phase gate between the two pairs, measuring one qubit in the X -basis, and performing a Hadamard rotation on the other. Although this simple method does not generalize to other graphs, the examples which we choose to give will be for linear cluster states, and hence this description is valid. For other graph states, the operation that we apply must project N qubits on a local site to 1 qubit, and is represented as

$$P = |0\rangle\langle 0|^{\otimes N} + |1\rangle\langle 1|^{\otimes N}.$$

For example, the required operations to create the pentagon of Fig. 1(a) are shown in Fig. 1(b).

A. Locally Reconstructible States

For a certain error model that we shall address (local Z -noise), we will be particularly interested in the restriction to a class of graph states which we call Locally Reconstructible (LR), defined as follows:

Definition 1. *Locally Reconstructible graph states are connected graph states for which there exists a non-trivial partitioning of the qubits into two parties such that neither party has more than one edge from each qubit crossing the partition.*

In order to prove that this class of states is non-trivial, we examine some of its properties in App. A. Importantly, this class includes all cluster states (d -dimensional cubes), GHZ states (one vertex with edges to all others), and graphs which are locally equivalent to the codewords of error-correcting codes such as the Shor-[[9,1,3]] code, the 5-qubit code (Fig. 1(a)) and the Steane-[[7,1,3]] code (Fig. 1(c)). Indeed, in both of these figures, we provide a partition that demonstrates the LR character of the corresponding graph.

We are not aware of this classification of graph states coinciding with any previous definition. For example, in Fig. 1 we provide two examples that show firstly that LR states are not necessarily two-colorable [12] (Fig. 1(a)) and, secondly, that not all two-colorable states are LR (Fig. 1(d)). In this case, for every possible partition, there is always a qubit that has at least two edges crossing the partition. One such partition is depicted in Fig. 1(d). Nevertheless, one can show that for all graphs of up to seven qubits the corresponding graph states are locally equivalent to LR states. Indeed, all the graphs in [21], which are used to categorize the local unitarily equivalent graphs of up to seven qubits, are LR. That is, one can reversibly transform pure graph states of seven or fewer qubits to LR states using local operations $\sqrt{K_i}$. For larger systems, there exist examples that are not locally equivalent to an LR graph. Specifically, the icosahedral graph (12 vertices, degree 5, Fig. 2) and its local equivalences form a collection of 54 graphs, none of which are LR. Since the operations $\sqrt{K_i}$ are Clifford operators, it remains a possibility that there are other local unitaries that could be applied which yield a different set of local equivalences [21, 23, 24].

III. PURIFICATION PROTOCOLS

The aim of a purification protocol is to take many identical copies of a noisy state ρ_G and produce a single, pure, copy $|\psi_G\rangle$. We consider that each qubit in the state ρ_G is held by a different party (Alice, Bob...), and that they hold the same qubit from every copy. The parties are restricted to applying Stochastic Local Operations and Classical Communication (SLOCC), which we initially assume to be perfect. These restrictions serve to illustrate the entanglement properties of ρ_G . There are also physically motivated systems where locality restrictions come into play, such as with quantum repeaters [9].

We assume that ρ_G is diagonal in the graph state basis, i.e.

$$\rho_G = \sum_{j \in \{0,1\}^N} \lambda_j Z_j |\psi_G\rangle\langle\psi_G| Z_j,$$

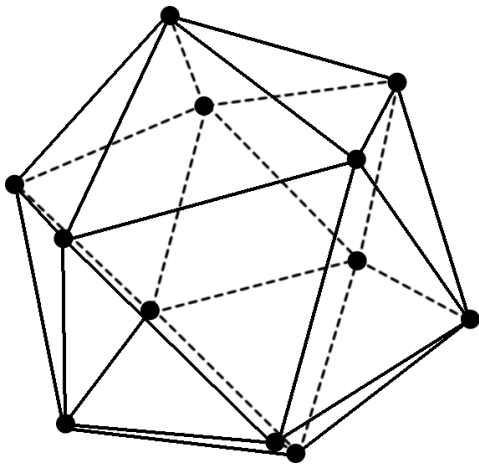


FIG. 2: The icosahedral graph, which is not equivalent to any LR states using the local operations $\sqrt{K_i}$.

where j indicates which of the N qubits a Z -rotation is applied to. As has previously been explained elsewhere (see, for example, [12]), any non-diagonal state can be made diagonal by SLOCC without changing the diagonal elements by probabilistically applying the stabilizers (with probabilities suitably chosen to negate the off-diagonal elements). The numbers $0 \leq \lambda_j \leq 1$ encapsulate all the information about the errors. We are assuming that we know all of these values i.e. we know the noise model, although it is not *strictly* necessary to know the error probability, p . Hence, without loss of generality, we assume that λ_0 is the largest element, since we wish to purify towards $|\psi_G\rangle$. This is the fidelity of the initial state ρ_G . If λ_0 were not the largest value, one could apply Z -rotations to make it the largest value, as these permute the diagonal elements.

In this paper, we are interested in proving universally applicable bounds. We shall define the *threshold fidelity* $f_{\text{threshold}}$ as the value of λ_0 below which purification is impossible, regardless of the protocol employed, for a specific noise model. All protocols have their own critical fidelity $f_{\text{crit}} \geq f_{\text{threshold}}$ below which that protocol does not work. Optimality of a protocol is proven when equality holds.

A. Genuine Multipartite Purification

In the following subsection, we will propose a protocol that is based on bipartite purification and thus is easily analyzed. Indeed, for some types of noise and classes of states, one can prove its optimality. However, this protocol will not perform well in general, and so when we are interested in other noise models, we are forced to resort to a multipartite purification protocol, such as the one described in [11, 12]. We refer to this specific protocol as the Genuine Multipartite Purification Protocol (GMPP).

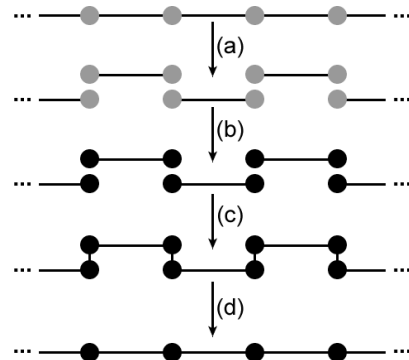


FIG. 3: The Divide and Rebuild Purification Protocol. We start with many copies of the noisy graph state. (a) We form two-qubit nearest-neighbor states (noisy) by performing Z -measurements. (b) Two-qubit states are purified (if possible). (c) Controlled-phase gates are applied between local qubits. (d) All qubits except one from each party are measured in the X -basis, leaving the remaining qubits in the purified state.

The GMPP is applied to two-colorable graph states, which are graph states where every qubit can be labelled as either A or B such that all edges connect an A and a B. The protocol proceeds by application of arbitrarily ordered sequences of two sub-protocols $P1$ and $P2$. Since Z -rotations form a complete basis for the graph state, the state can be labelled by vectors μ_A and μ_B , specifying which A or B qubits, respectively, have Z -rotations applied to them. The action of the two protocols is

$$P1 : \lambda_{\mu_A, \mu_B} = \sum_{\nu_B} \lambda_{\mu_A, \nu_B} \lambda_{\mu_A, \mu_B \oplus \nu_B}$$

$$P2 : \lambda_{\mu_A, \mu_B} = \sum_{\nu_A} \lambda_{\nu_A, \mu_B} \lambda_{\mu_A \oplus \nu_A, \mu_B}$$

which then have to be renormalized. Both are realized by post-selecting on particular measurement results, which means that the rate of purification decreases exponentially with the number of qubits present. The application of the GMPP is challenging to analyze due to the arbitrary choice of the sub-protocols $P1$ and $P2$ at each step. In general, we resort to numerical exploration which, with finite computational resources, can never tell us precisely how close the GMPP comes to any upper-bound. Another multipartite purification protocol has recently been proposed [15], which is easier to analyze for a range of errors, and achieves a superior purification rate. However, the critical fidelities at which it works are larger than for the GMPP, so little benefit can be derived from comparing them to the threshold fidelities which we calculate. Other recent work [13, 14] has described protocols which are not limited to two-colorable states.

B. Bipartite-based Purification

The second purification protocol which we will analyze is certainly not new (see, for example, [10, 16, 25]), but

its simplicity enables the derivation of rigorous results. To implement the protocol (Fig. 3), we initially measure the qubits of the graph state in the Z -basis until we are left with a single two-qubit state ρ_2 . Many copies of this state are then used to purify, if possible, a Bell pair $|\psi_2\rangle$. By performing Z -measurements on different sets of qubits, different Bell pairs are generated. Once we have a Bell pair for every edge in the graph, we can locally reconstruct the state, e.g. by applying controlled-phase gates and X -measurements. The conditions under which $\rho_2 = \text{diag}(\lambda_{00}, \lambda_{01}, \lambda_{10}, \lambda_{11})$ can be purified to $|\psi_2\rangle$ are well-known [7, 8],

$$\lambda_{00} > \frac{1}{2}, \quad (2)$$

and have been shown to be optimal using the positive partial transpose condition [26, 27]. Hence, we only have to relate λ_{00} to the values of λ_j of the original state, ρ_G . We refer to this protocol as the Divide and Rebuild Purification Protocol (DRPP).

In [20], we considered the rate of purification for the DRPP, which is applicable whenever it is the optimal protocol. The rate of purification, R_ψ , for the state $|\psi\rangle$ was described in terms of the rate of purification of a Bell state, R_2 , taking the standard definition of rate,

$$R_\psi = \frac{\# \text{ of copies of } |\psi\rangle \text{ produced}}{\# \text{ of copies of } \rho \text{ consumed}}.$$

This allowed us to bound the rate of purification by

$$R_2 \geq R_\psi \geq \frac{R_2}{N_{\text{geo}}}.$$

where N_{geo} is a small geometric factor determined by the graph. This rate is a vast improvement over the GMPP, although other protocols have better rates at the cost of being less robust [15]. For d -dimensional cluster states, it was shown that the geometrical factor $N_{\text{geo}} = 3d^2$ is independent of the size of the graph. A similar argument can be applied to general graph states, and yields an upper bound

$$N_{\text{geo}} \leq \min \left(2(D_G - 1)D_G + 1, \binom{N}{2} \right)$$

where D_G is the maximum degree of G i.e. no vertex has more than D_G edges. This does not coincide with the result for cluster states because we used knowledge of the geometry of cluster states to optimize our use of resources.

C. Upper-Bound to the Purification of Multipartite States

The intention of this paper is to make statements about when purification is impossible for all protocols. To provide such a proof, we consider two parties Alice and Bob, each locally handling many qubits. The operations they perform are more general, but include, multipartite operations.

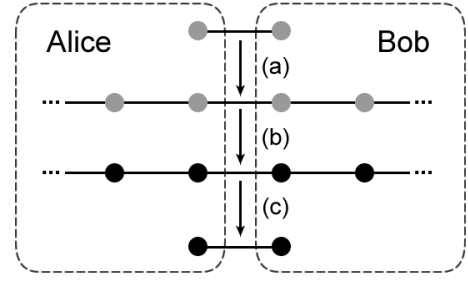


FIG. 4: If we assume the existence of a purification protocol for the multipartite state, then this implies that we can purify the two-qubit state. (a) Alice and Bob take the two-qubit state and reconstruct the noisy graph state. (b) This state is purified. (c) All extra qubits are measured out to return the original pair, now pure.

Theorem 1. Consider the scenario where we wish to purify a two-qubit state ρ_2 . Provided that many copies of ρ_2 can be converted by SLOCC into a noisy graph state ρ_G held by the two parties, then if purification of ρ_2 is impossible, so is purification of ρ_G .

Proof. The veracity of this theorem is shown by contradiction. We assume that purification of ρ_G is possible by some protocol. From the condition of the theorem, we can start with ρ_2 and locally convert it into ρ_G by employing extra qubits. By assumption, there exists a protocol that can purify this state, leading to the pure state $|\psi_G\rangle$. This can be converted into a maximally entangled two-qubit state by projecting out the additional qubits with local Z -measurements. Hence, ρ_2 can always be purified if ρ_G can be purified. If we know that ρ_2 cannot be purified, we have a contradiction, and the initial assumption must be false. These steps are depicted in Fig. 4. \square

A corollary is that if the state ρ_G is described by a parameter p indicating the probability of an error occurring, this theorem gives an upper-bound on the value of p such that ρ_G can be purified. This could alternatively be viewed as a lower-bound on the required fidelity of the state ρ_G . We choose to refer to it as an upper-bound.

Little is known about the conversion between bipartite (multi-level) mixed states $\rho_2^{\otimes n} \rightarrow \rho_G$ [28], as required for the local reconstruction condition of Theorem 1. Thus, we have to examine different noise models on a case-by-case basis, which we do in Sec. IV. For LR graphs, such as Fig. 5(a), local reconstruction simply involves replacing each link across the Alice/Bob partition by a single copy of the two-qubit state. However, for non-LR graphs, such as Fig. 5(c), this is not possible because two links need to be replaced which connect to a single qubit. While reconstruction is still possible in these cases, it generally means an increase in the local error probability, which becomes correlated in a different way to the errors in the

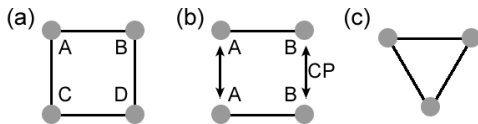


FIG. 5: (a) Square graph shared between 4 parties. (b) Alice and Bob can locally reconstruct the square graph using two copies of ρ_2 , and applying controlled-phase gates between them. (c) The triangular graph is the simplest configuration for which the optimality proof fails.

rest of the graph. This makes analysis more difficult, weakening the bounds that one can derive.

Theorem 1 can be generalized by making two further observations. Firstly, it is not necessary to restrict to a bipartite state ρ_2 , since any state which can be locally converted into the state ρ_G could be used. However, the only existing optimality conditions apply to two-qubit states. Secondly, the states that we use need not be graph states, it is just that the formalism of graph states guarantees that we can convert $|\psi_G\rangle$ into $|\psi_2\rangle$. In the general case, we should be able to perform measurements on $|\psi_G\rangle$ which return a pure 2-qubit state with non-zero entanglement, and can subsequently be distilled to a maximally-entangled state. In Sec. V, we apply this method to the concrete example of a valence bond state.

D. Comparison to the positive partial transpose condition

Essential to the application of Theorem 1 is the knowledge of when a two-qubit state can be purified, which can only happen if there is non-zero distillable entanglement between the two parties. We can therefore interpret Theorem 1 as stating that purification of a multipartite state is impossible if there is a bipartite split for which there is no distillable entanglement. Following this interpretation, we can describe existing multipartite purification protocols as examples of bipartite purification protocols which use separable operations. In particular, we observe that the operation of the GMPP is closely related to the protocol of [29]. The action of this high-dimensional bipartite purification protocol can be analyzed [30], enabling rigorous comparison between its performance and the upper-bounds calculated in this paper.

With the aforementioned entanglement interpretation, it is simple to see that Theorem 1 is a constructive statement that can sometimes be applied to discover if a state can be written in the form

$$\sum_i p_i \rho_i^A \otimes \rho_i^B.$$

Consequently, we should expect similar results to those of [19], where the positive partial transpose (PPT) condition is applied to bipartite groupings of multipartite states. However, in [19], extra depolarization steps are

applied which tend to remove entanglement from the system and, consequently, tight bounds are not expected.

In general, how should our technique compare to the PPT condition, if one does not introduce additional depolarizing steps? As expressed in terms of a reconstruction from two-qubit states, our upper bounds are strictly weaker than PPT. We can see that this is the case because starting from any two-qubit state which is separable (for which the PPT condition is necessary and sufficient), and applying SLOCC results in a state which necessarily has PPT i.e. is separable, and purification is impossible. However, there also exist states with PPT which cannot be generated from two-qubit separable states, which are known as bound-entangled states. Therefore our condition is strictly weaker than PPT.

Nevertheless, our condition has two major benefits. Firstly, as already indicated, we need not be restricted to reconstructing from two-qubit states. In particular, *if* there exist bound entangled states with non-PPT (this still remains an open question), then using these as a basis for reconstruction yields a stronger bound on purification than the PPT condition can provide. Secondly, our technique is constructive, which eases its application in many scenarios, including the situation where the gates applied during the purification procedure are faulty (this will be explored in a later paper).

IV. UPPER-BOUNDS FOR VARIOUS ERROR MODELS

Given Theorem 1, it is interesting to apply the method to different types of noise, yielding bounds on when noisy states are not purifiable. It may not be possible to attain these bounds with purification protocols, and we will be able to demonstrate that the DRPP does not always achieve them. Numerical studies of the GMPP indicate a much tighter match in performance, although given the asymptotic approach to the bound, and the existence of strong local attractors, in most cases it is impossible to precisely verify whether they match.

A. Local Z-Noise

A straightforward application of our theorem comes when considering local Z-noise. While a very restrictive noise model, it has two physical motivations, namely that the thermal state of the Hamiltonian in Eqn. (1) is equivalent to the ground state with local Z-noise, and that Z-noise is a significant source of error in some experimental implementations, such as optical lattices. Moreover, as we will see, within our treatment this type of noise is the worst-case noise, giving the lowest probability threshold of all the local noise models considered here.

We assume that a Z-error occurs on each qubit independently, with probability p . When we restrict to LR states, local reconstruction follows by replacing any links

across the bipartition with noisy two-qubit states. The structure of the class guarantees that the only subsequent operations that we need to perform are local controlled-phase gates between qubits. Since these gates commute with Z -errors, then starting with a two-qubit state, a many-qubit state can be built with the same error probability. The two-qubit state cannot be purified if

$$(1-p)^2 < \frac{1}{2},$$

so this must hold for all LR states.

Similarly, since Z -measurements commute with the Z -errors, we can show that the DRPP can purify the whole state provided

$$(1-p)^2 > \frac{1}{2}.$$

Thus, the protocol is optimal, with a threshold probability of $p = 1 - 1/\sqrt{2} \approx 0.29$. Equivalently,

$$f_{\text{threshold}} = f_{\text{crit}} = (1-p)^N = \frac{1}{2^{N/2}}. \quad (3)$$

This provides a useful benchmark to test other purification protocols, such as the GMPP (see Sec. IV D). Note that the DRPP can purify all graph states with the same critical fidelity.

Local Z -noise also corresponds to the thermal state of the Hamiltonian in Eqn. (1), and provided we set $J_i = \Delta/2$, the local error probability is the same at each site,

$$p = \frac{e^{-\beta\Delta}}{1 + e^{-\beta\Delta}}$$

where the temperature T is encapsulated in the parameter $\beta = 1/(k_B T)$. Given our proof of optimality, this can be phrased as a critical temperature,

$$T_{\text{crit}} = \frac{-\Delta}{\ln(\sqrt{2}-1)}, \quad (4)$$

which corresponds to one of the bounds found in [16], as one expects since the argument of [16] also involves

the breaking of cluster states into two-qubit states. As discussed in [20], it should be possible to probe this temperature with existing experimental implementations.

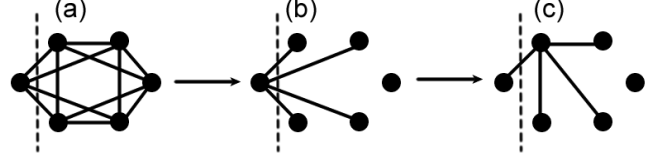


FIG. 6: (a) Take a general graph and bipartition it with a single qubit on one side. (b) Apply local controlled-phase gates along all edges. (c) Apply unitaries \sqrt{K} to change the central node of the GHZ state. Theorem 1 can now be applied to obtain upper bounds.

Thresholds can also be derived for arbitrary graphs by first applying appropriate transformations. Select from a particular graph, G , a single qubit which has the minimum number of nearest neighbors (minimum degree) D_{\min} , which we take to constitute a partitioning of the graph. We now give a reversible procedure which is local to this partitioning to convert the state into a GHZ state which is LR across the partition. By applying controlled-phase gates along all edges that are not connected to our chosen qubit (remember that these gates commute with the Z -noise), we are left with a $(D_{\min} + 1)$ -qubit GHZ state as depicted in Fig. 6(b). However, the links across the partition are not the same as for an LR state. To account for this, we apply local unitaries $\sqrt{K_i}$ on our chosen qubit and one of its neighbors, performing the transformation depicted in Fig. 6(c). These local unitaries transform the noise model from local Z -errors to an X -error on the original qubit, a Y -error on the center of the GHZ state, and Z -errors everywhere else. The corresponding density matrix can be written in the graph state basis as

$$\rho = \sum_{j \in \{0,1\}^{D_{\min}-1}} (1-p)^{w_j} p^{w_j} \text{diag}((1-p)^{D_{\min}+1-2w_j}, p(1-p)^{D_{\min}-2w_j}, p^{D_{\min}+1-2w_j}, (1-p)p^{D_{\min}-2w_j}) \otimes |j\rangle\langle j|, \quad (5)$$

where w_j is the binary weight of j . These diagonal elements $\langle j|\rho|j\rangle$ are indexed by a number $j \in \{0,1\}^{N-1}$, where the i^{th} bit indicates whether a Z -error has occurred on the i^{th} qubit relative to the desired pure state $|\psi_G\rangle$. The most entangled pair of qubits is given by $j = 0$, so we define

$$\rho_2 = \frac{\text{diag}((1-p)^{D_{\min}+1}, p(1-p)^{D_{\min}}, p^{D_{\min}+1}, (1-p)p^{D_{\min}})}{(1-p)^{D_{\min}} + p^{D_{\min}}}. \quad (6)$$

From this state, the entire state ρ in Eqn. (5) can be re-

constructed. Hence, if ρ_2 becomes separable, purification

must be impossible, i.e. if

$$2(1-p)^{D_{\min}+1} \leq (1-p)^{D_{\min}} + p^{D_{\min}}.$$

For $D_{\min} = 1$, we recover the bound for the LR graphs as expected. However, LR graphs need not have $D_{\min} = 1$, proving that this bound is not always tight. For the triangular and icosahedral graphs, these calculated threshold probabilities are $p = 0.352$ (which the GMPP appears to numerically saturate, thereby exceeding the DRPP) and $p = 0.413$ respectively. As $D_{\min} \rightarrow \infty$, $p \rightarrow \frac{1}{2}$. The bounds given by [19] in this case also show that purification is impossible if $p > \frac{1}{2}$, but make no tighter claims.

B. Maximally (Global) Depolarizing Noise

In the previous subsection, we proved optimality of purification for local Z -noise. The local unitary equivalence of graphs can provide similar bounds for a range of other local noise models. It is now interesting to examine the case of correlated noise, and to derive bounds in this context. We will prove bounds for all graph states by initially restricting to linear cluster states. Choosing the noisy state to be purified as the maximally depolarized state of an N -qubit linear graph state $|\psi_G\rangle$,

$$\rho_N = \frac{\mathbb{1} + x|\psi_G\rangle\langle\psi_G|}{2^N + x},$$

we give an inductive proof which shows how to locally create $\rho_N(x)$ from $\rho_{N-1}(x)$. If we take $\rho_{N-1}(x)$ and add an extra qubit to it, then the density matrix takes the form

$$\rho'_{N-1}(x) = \text{diag}(1+x, 0, 1, 0, 1, 0, \dots, 1, 0)/(2^{N-1} + x).$$

Upon application of a Z -rotation to the new qubit (the least significant bit of i), the zeros and non-zeros swap. Further Z -rotations on the other qubits can permute the position of the $1+x$ term. Taking each of these with probability $(1-p)/2^{N-1}$, or $\rho'_{N-1}(x)$ with probability p , we are left with the density matrix

$$\frac{p}{2^{N-1}+x} \text{diag}(1+x, 0, 1, 0, 1, 0, 1 \dots) + \frac{1-p}{2^{N-1}} \text{diag}(0, 1, 0, 1, 0, 1 \dots)$$

This can be forced to take the form of $\rho_N(y)$ by selecting

$$p = \frac{2^{N-1} + x}{2^N + x}.$$

and $x = y$. Consequently, the threshold value of $x = 2$ for the bipartite case holds for all N , and the threshold fidelity is

$$f_{\text{threshold}} = \frac{3}{2^N + 2}. \quad (7)$$

By allowing an arbitrary two-qubit density matrix of the form $\rho_2 = \text{diag}(\frac{1}{2}, a, b, \frac{1}{2} - a - b)$, it is possible to prove that no better bound can be given by this method.

In App. B, we calculate the performance of the DRPP, which performs very poorly in the presence of correlated noise, being unable to purify if $f < 1/3$. For $N = 2, 3$, the GMPP manages to saturate this bound. However, for $N > 3$, we have been unable to find suitable repetitions of $P1$ and $P2$ which purify if $f < 1/2^{N/2}$. This is because the maximally mixed state of one set of errors (i.e. errors on just the ‘A’ qubits, with pure ‘B’ qubits), which has fidelity $1/2^{N/2}$, is a strongly attracting fixed point. In App. C, we apply the results of [30] to show that for the closely related protocol of [29] when the qubits are partitioned into two equally sized sets, $f = 1/2^{N/2}$ is indeed a fixed point.

The threshold fidelity for GHZ states is also given by Eqn. (7), since the above proof also holds for all states with a single edge across the bipartite division. The advantage is that the two potential fixed points in fidelity ($1/2$ and $1/2^{N-1}$) are different from those of a linear chain. Moreover, the smaller of these is below the threshold fidelity, and is trivially avoided. For example, for $N = 5$, purification of $x \geq 2.024$ is possible using the GMPP. Given the anticipated asymptotic approach to the critical fidelity, the GMPP seems to saturate the bound of Eqn. (7). The threshold fidelity for GHZ states coincides precisely with that of [19], although our chosen parameterization of the state provides a more convenient condition for purification.

It is now possible to follow an identical protocol to Fig. 6 in the case of maximally depolarizing noise to prove that all graphs are subject to the bound in Eqn. (7). This follows trivially from the observation that the application of controlled-phase gates and local unitaries $\sqrt{K_i}$ do not change the noise model, only the underlying graph. Once we have a GHZ state with a suitable partition, the above derivation applies.

C. Local Depolarizing Noise

In addition to local Z -noise, a range of other local noise models could be considered. One such model is where the type of local unitary that is applied is not known, but it occurs with probability p . This is equivalent to local depolarizing noise occurring with a probability $4p/3$,

$$\begin{aligned} \mathcal{E}_p^i(\rho) &= (1-p)\rho + \frac{p}{3}(X_i\rho X_i + Y_i\rho Y_i + Z_i\rho Z_i) \\ &= \left(1 - \frac{4p}{3}\right)\rho + \frac{4p}{3}\frac{1}{2}\mathbb{1}_i \otimes \text{Tr}_i(\rho). \end{aligned}$$

To derive a threshold, it is possible to follow a similar process to the previous subsection. Of critical importance to calculating a tight bound is the optimal selection of the two-qubit state to use across the partition. When considering linear graphs, this state varies with the length of the chain. To illustrate this, we shall discuss the case of 3 qubits in more detail. The target density matrix, written in the graph state basis, takes the form

$$\rho = \text{diag}(a, b, c, b, b, b, b, b),$$

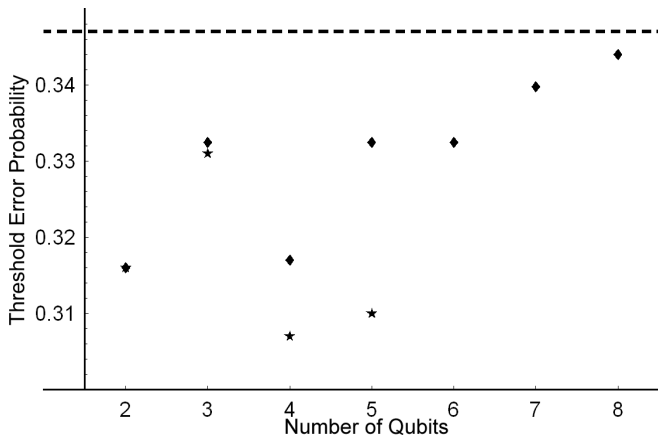


FIG. 7: Diamonds indicate the probability of a local depolarizing error above which purification of a linear chain is impossible. The dashed line indicates a bound below which all such probabilities must lie. Stars indicate values for which purification can be achieved with the GMPP.

where a , b and c are specified in terms of p . This can be divided into a probabilistic mixture of two components,

$$\begin{aligned} \rho &= \text{diag}(a, 0, c, 0, b, 0, b, 0) + \text{diag}(0, b, 0, b, 0, b, 0, b) \\ &= \text{diag}(a, c, b, b) \otimes |0\rangle\langle 0| + \frac{b}{4} \text{diag}(1, 1, 1, 1) \otimes |1\rangle\langle 1|. \end{aligned}$$

The second of these is a maximally mixed state on the two qubits that have an edge crossing the bipartite partition, perfectly connected to a third qubit (with a Z -rotation). It is always possible to prepare this, so our only condition relates to the creation of the first term, which is a two-qubit state $\text{diag}(a, c, b, b)/(a + 2b + c)$ perfectly connected to the third qubit. This is the form of two-qubit state that we choose to use, and purification is impossible if $a/(a + 2b + c) \leq \frac{1}{2}$. Upon evaluation of a , b and c , this gives

$$27 - 126p + 156p^2 - 64p^3 \leq 0,$$

from which we find the threshold probability of 0.332. A similar process can be adopted for all linear graphs, and the results are presented in Fig. 7. In App. B, we derive the performance of the DRPP, which fails to achieve these bounds. For 2 qubits, the GMPP is the same as the protocol in [7], and therefore achieves the two-qubit bound of 31.7% asymptotically. For 3 qubits, the GMPP comes close to matching these bounds, purifying at 33.1%. However, for $N \geq 4$, the strongly attracting fixed point of $f = 1/2^{\lceil N/2 \rceil}$ occurs close to the threshold probability. This makes numerical analysis particularly challenging in these cases.

These bounds exceed the bound for local Z -noise because for the graph states, Z -noise forms a complete basis, whereas the other errors do not. Consequently, when two errors coincide, they might cancel, and hence it may become slightly easier to purify the state. For example,

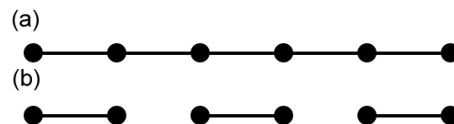


FIG. 8: For the GMPP, purification is geometry independent. This means that the purification regimes for the two depicted states are identical.

the purification condition for two qubits subject to local depolarizing noise is $(1 - p)^2 + p^2/3 > \frac{1}{2}$ instead of $(1 - p)^2 > \frac{1}{2}$ (Z -noise), where the extra term comes from cancellation of coinciding errors.

A general bound for a chain of arbitrary length can be obtained by demanding the conditions under which we can create a particular N -qubit state, where only the first $N - 1$ qubits are noisy. Provided $N \geq 3$, we can create a chain of arbitrary length $M \geq N$ by adding $M - N$ qubits to the end of the chain, along with the required noise. This bound must be non-increasing with increasing N . Selecting $N = 10$, we find that purification is impossible for all chains of ten or more qubits if $p > 0.347$. Consequently, the threshold probability must tend towards a constant, as observed numerically for the GMPP in [12]. The optimal protocol must also tend to a constant because of the constant lower-bound provided by the DRPP (App. B).

In comparison to linear or GHZ states, the case of the Steane $[[7,1,3]]$ code is slightly more involved because we need three two-qubit states to cross the bipartite split. However, all three become separable at the same threshold probability of $p = 0.403$. Numerically, we find that the GMPP becomes trapped in the fixed point of $f = 1/2^4$.

D. Analysis of the GMPP

To date, evaluation of the performance of the GMPP has resisted analytic techniques, and has instead relied on numerical evaluation, as we have used in this section. While we have observed a close relationship between the GMPP and the analytic bipartite purification protocol of [29, 30], the direct proof of any connection still remains an open problem. However, we are able to make progress in proving the purification regime for the GMPP in certain special cases. Given this, it becomes interesting to compare the performance of the two purification protocols, the DRPP and the GMPP. Earlier in this section, we have provided several examples where the GMPP outperforms the DRPP. In this subsection we will present our analysis of the GMPP, and construct an example in which the GMPP is provably sub-optimal, being outperformed by the DRPP. This yields an interpretation as to why the GMPP can get trapped in fixed points for certain error models.

We proceed by realizing that the sub-protocols of the

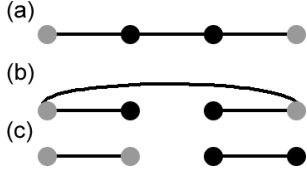


FIG. 9: Consider purification of the graph in (a) where gray circles denote qubits with Z -errors with probability p , and black circles are pure qubits. For the GMPP, purification of parts (a), (b) and (c) are identical. (b) provides an upper bound of $p = 30\%$ for the GMPP, and (c) proves that this can be achieved. The DRPP can always purify (a) for arbitrary p .

GMPP depend only on the diagonal elements of the density matrix, and not the underlying geometry, other than the numbers of qubits of each color in the two-colorable graph. This means that the purification regimes of the graphs depicted in Fig. 8 are identical. Hence, one can restrict to considering purification of the graph in Fig. 8(b). Further, if we assume that the noise is not correlated between the pairs, and that it is identical for each pair, then the GMPP is exactly the same as the DRPP, except that purification of the pairs occurs in parallel instead of independently, leading to the observed reduction in purification rate. Given that we can derive the performance of the DRPP, we can deduce the performance of the GMPP in this case and, consequently, in the case of more complex graphs such as Fig. 8(a). One such example of noise is local Z -noise, instantly proving that the GMPP is optimal for local Z -noise on LR graphs.

The geometry independence of the GMPP means that it can purify all two-colorable graphs with local Z -noise with the same critical probability. This includes graphs such as Fig. 1(d), for which our analysis gives a threshold probability of $p = 0.352$. We interpret the failure to saturate this bound as the geometry independence of the GMPP causing it to become trapped by local fixed points.

In Fig. 9, we consider purification of a linear graph where two of the qubits have a Z -error with probability p , and the other two qubits are pure. Given the geometry independence of the GMPP, its critical probability is the same as for Fig. 9(b). As we have seen in Sec. IV A, purification of this graph must be impossible if $p \geq 1 - 1/\sqrt{2}$. Consequently, the GMPP cannot purify Fig. 9(a) if $p \geq 1 - 1/\sqrt{2}$. A similar manipulation to Fig. 8 yields Fig. 9(c), which can also be used to show that purification below this critical probability is possible (application of purification to the pure pair leaves it pure, so we only have to purify the noisy pair, for which the GMPP is the same as the optimal two-qubit protocol).

Now consider applying the DRPP to the original chain (Fig. 9(a)). Each of the three edges to be purified can always be purified – one is already pure and the other two only have two diagonal elements to their density ma-

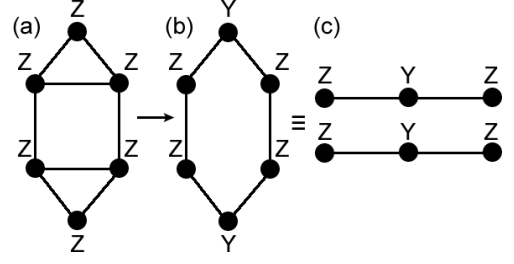


FIG. 10: Local operations can convert local Z -noise on graph (a), which is LR, into a two-colorable graph (b). The GMPP can purify this if it can purify (c). However, this is not the same constraint as the ability to purify a single copy of the three-qubit state.

trices, so can always be purified. Hence, the state in Fig. 9(a) can always be purified. This proves that the GMPP is sub-optimal and that in some circumstances the DRPP out-performs it.

There are certain pitfalls associated with this analysis of the GMPP that we will illustrate with an example. Consider the purification of the triangular graph with local Z -noise, for which our upper bound has predicted the impossibility of purification if $p > 0.352$. The state can be transformed into a linear graph by local operations where the errors are now Z, Y, Z , and since this graph is two-colorable, the GMPP can be applied. Numerically, it appears to saturate our bound. We can now consider the purification of the LR state depicted in Fig. 10(a). With local Z -noise, we already know that purification is impossible if $p > 0.3$. However, we can apply local operations to form a two-colorable state, and subsequently apply the geometry independence of the GMPP to see that purification of this state is equal to the parallel purification of two of the triangular graphs, and hence it appears that it should have the same purification regime. Clearly, there is a discrepancy. This is resolved by observing that the performance of the purification in parallel is not identical to two independent purifications in this case because there is an asymmetry between the $P1$ and $P2$ protocols i.e. the parallel application requires $P1' = P1 \otimes P1$ and $P2' = P2 \otimes P2$, where $P1$ and $P2$ are the protocols on the triangle, whereas the GMPP applies $P1' = P1 \otimes P2$ and $P2' = P2 \otimes P1$.

V. PURIFICATION OF VALENCE BOND STATES

Using a combination of the DRPP and Theorem 1, we have proved that for local Z -noise, and some other types of local noise, there is a threshold error probability below which purification is possible, and above which purification of graph states is impossible. However, there is no need to restrict to graph states. By making use of the valence bond formalism, we will now construct an example of a state which is not a graph state, but can be optimally

purified by the DRPP.

A general valence bond state [22, 31, 32, 33] can be described by employing a D -dimensional maximally entangled state between each nearest-neighbor of a graph. Each local party then projects down to a d -dimensional system with a specific projector. If we allow $D = 2^{N/2}$, then any N -qubit state can be described by this formalism [31]. The class of translationally invariant states can be described efficiently, using a fixed D . These D -dimensional maximally entangled states can be formed from $\log_2(D)$ Bell states. We are solely interested in constructing a simple example to demonstrate the general properties. As such, we shall restrict to $D = d = 2$ and to a linear graph of 3 qubits. This contains all the essential properties of valence bond states and, consequently, we expect that generalizations will follow in a straightforward manner.

The purification protocol follows the concept of the DRPP, as already outlined. Our initial state is described by two maximally entangled states $|\phi\rangle$, joined by a single projector P_0 , acting on qubits 2 and 3.

$$|\psi_{\text{initial}}\rangle = \mathbb{1} \otimes P_0 \otimes \mathbb{1} |\phi\rangle_{12} |\phi\rangle_{34}$$

If local Z -noise affects our state, then we apply Z -measurements to all the qubits apart from a single pair, which should retain some entanglement. Since the noise commutes with the measurement, it suffices to describe what happens to the pure state,

$$\begin{aligned} |\psi_2\rangle |0\rangle &= \frac{1}{2} \mathbb{1} \otimes P_0 \otimes |0\rangle\langle 0| \left(\sum_i |i\rangle |i\rangle \right)^{\otimes 2} \\ &= \frac{1}{2} \mathbb{1} \otimes P_0 \otimes \mathbb{1} \left(\sum_i |i\rangle |i\rangle \right) |0\rangle |0\rangle, \end{aligned}$$

where we have assumed outcome $|0\rangle\langle 0|$ from the Z measurement. Using many copies, the state $|\psi_2\rangle$ with local Z -noise can be purified to a two-qubit maximally entangled state, $|\phi\rangle$. We repeat this for each edge of the graph, and the pure state $|\psi_{\text{initial}}\rangle$ is recovered by applying local projectors P_0 to each vertex. We can express the projector P_0 as

$$P_0 = \sum_{i,j,k} \alpha_{j,ik} |j\rangle \langle i| \langle k|$$

so that α^k constitutes a $d \times d$ matrix, $\langle j| \alpha^k |i\rangle = \alpha_{j,ik}$. Note that this definition does not coincide with the standard matrix product state definition of these matrices (where $\langle j| \alpha^k |i\rangle = \alpha_{k,ji}$).

For the optimality proof, we need to start with the state $|\psi_2\rangle$ and show how to reconstruct $|\psi_{\text{initial}}\rangle$. We do this by locally introducing a maximally entangled state $|\phi\rangle$, and applying a projector P_1 .

$$\mathbb{1} \otimes P_1 \otimes \mathbb{1} |\psi_2\rangle |\phi\rangle = |\psi_{\text{initial}}\rangle. \quad (8)$$

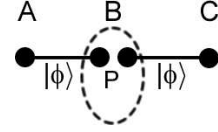


FIG. 11: The valence bond state that we wish to purify is generated from two maximally entangled states $|\phi\rangle$, and a projector P applied between them.

If Z -noise is present on $|\psi_2\rangle$, then it must reappear on $|\psi_{\text{initial}}\rangle$ when we apply P_1 ,

$$(\mathbb{1} \otimes P_1 \otimes \mathbb{1}) \cdot (\mathbb{1} \otimes Z \otimes \mathbb{1} \otimes \mathbb{1}) |\psi_2\rangle |\phi\rangle = \mathbb{1} \otimes Z \otimes \mathbb{1} |\psi_{\text{initial}}\rangle. \quad (9)$$

P_1 can be described analogously to P_0 ,

$$P_1 = \sum_{i,j,k} \beta_{j,ik} |j\rangle \langle i| \langle k|$$

which, through Eqn. (8), allows us to show that

$$\beta^i \alpha^0 = \alpha^i.$$

Subsequent expansion of Eqn. (9) enables the derivation of a simple condition for when the reconstruction can be performed, and hence when the optimality proof holds,

$$[\beta^i, Z] \alpha^0 = 0. \quad (10)$$

This does not hold for all valence bond states, but we can construct examples when it does. In the case where α^0 and α^1 are invertible, we find that $\alpha^0(\alpha^1)^{-1}$ must be diagonal. Applying the optimality proof on both edges of the graph provides a symmetry between the elements $\alpha_{j,ik}$ and $\alpha_{j,ki}$. This leads to a final form of the projector

$$P_0 = \begin{pmatrix} \frac{\alpha_{0,01}\alpha_{0,10}}{\alpha_{0,11}} & \alpha_{0,01} & \alpha_{0,10} & \alpha_{0,11} \\ \frac{\alpha_{1,01}\alpha_{1,10}}{\alpha_{1,11}} & \alpha_{1,01} & \alpha_{1,10} & \alpha_{1,11} \end{pmatrix}.$$

In the special case of $\alpha_{1,11} = e^{i(\theta_1+\theta_2)}$, $\alpha_{1,10} = e^{i\theta_2}$, $\alpha_{1,01} = e^{i\theta_1}$ and $\alpha_{0,11} = \alpha_{0,10} = \alpha_{0,01} = 1$, we recover the weighted graph states [23, 34] and the cluster state ($\theta_1 = \theta_2 = \pi$). Weighted graph states are identical to the graph states that have been discussed so far except that to construct the state, instead of a controlled- Z gate between nearest-neighbors initially in $|+\rangle$, a controlled-phase gate of arbitrary phase is used. This means that all the relevant actions continue to commute with Z -errors, and we recover trivially the previous optimality proof, providing a useful verification of these results. Since the weighted graph states have an exponentially decreasing localizable entanglement length [31, 35], the general solutions, as described by P_0 , are expected to have finite localizable entanglement length.

VI. CONCLUSIONS

In this paper, we have described a method which proves that certain noisy multipartite states cannot be

purified. For the case of LR states subject to Z -noise with probability p , we have been able to show that for $p > 30\%$, purification is impossible, and that all other states can be purified i.e. we have demonstrated optimality of the purification protocol.

Numerical evidence indicates that the GMPP [11, 12] is optimal (in terms of the states that can be purified) for a large range of different errors, including local errors such as Z -noise (for which we have *proven* optimality), and non-local errors such as maximally depolarizing noise. There are cases where the GMPP is not optimal and in all such cases, we have observed that the protocol gets trapped by strong local attractors with fidelities $\frac{1}{2^n}$ and $\frac{1}{2^m}$, where the two-colorable state has n qubits of one color, and m qubits of the other. These can often be interpreted as being due to the geometry independence of the GMPP. This also coincides with the results that can be derived for the bipartite purification protocol (applied to systems of arbitrary dimension) in [29, 30]. The purification of the noisy graph in Fig. 9(a) provides proof that this is a real phenomenon, and not just an artefact of finite computational resources – the GMPP has a critical probability for purification, but other protocols can always purify the graph.

Not only have we demonstrated the optimality of purification of some graph states, but have also provided an example of a valence bond state which can be optimally purified, thus demonstrating the general utility of our method.

In forthcoming work, we shall examine how our upper-bound method can be applied to the situation where the gates used during the purification are also faulty, which is a major advantage of our constructive approach. This has potential implications for upper bounds on fault-tolerant thresholds. Interesting extensions of this work could involve taking what we have learnt about the performance of the GMPP and trying to improve it. In particular, we have demonstrated that one should take into account both the geometry of the state and the noise model when constructing a purification protocol, not just the noise model (in the case of the GMPP) or the geometry (in the case of the DRPP). A combined approach, based on the stabilizers of the state, but allowing asymmetry between the terms, appears to be the most sensible approach.

Acknowledgments

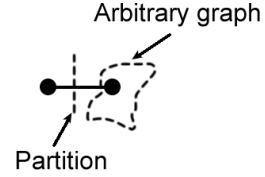
We would like to thank Hans Briegel, Wolfgang Dür, Robert Raussendorf and Peter Rohde for helpful conversations. This work was supported by EPSRC, Clare College, Cambridge and the Royal Society.

APPENDIX A: ANALYSIS OF LR CLASS

Given our rather abstract definition of the LR class, it is a worthwhile exercise to verify that it is a non-trivial class.

1. Graphs of Maximum Degree 3

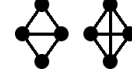
Let us consider all possible graphs which have a maximum number of nearest neighbors (degree) equal to 3 or less. If one of the qubits in the graph has degree 1, then there exists a trivial partition that shows that the state is LR.



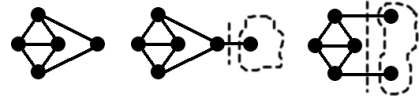
All other graphs must contain a loop. If we take the smallest loop in the graph, then the qubits in this loop already have at least two neighbors. We start by taking the triangle, a loop of 3 qubits. With no additional connections, this state is non-LR.



If we add one extra qubit, then by connecting it to two or three qubits in the triangle, the state is non-LR.

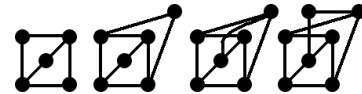


When the extra qubit is only connected to two qubits, there are two further links that could be added to any arbitrary structure. If they are not connected to the same qubits, these two links provide an LR partition.



The only remaining structure is where all three links from the triangle are connected to some arbitrary graph, but are not incident on the same qubit. These extra links must provide an LR partition.

We now continue this argument to loops of 4 qubits. Any structure which we add that generates a triangle has, of course, already been dealt with. This only leaves four examples which are non-LR.



Finally, for larger loops, there is no way of creating a graph that is non-LR without forming smaller loops first. Consequently, for graphs of maximum degree 3, there are only 8 graphs which are non-LR. It can be verified that the latter are locally equivalent to LR states.

N	LR states	All graph states
3	7	8
4	53	64
5	788	1024
6	22204	32768
7	1148781	2097152

TABLE I: Comparison of the number of LR states of N qubits and the total number of graph states. Note that we have included the completely separable state in the set of LR states.

2. Size of LR Class

It is important to answer the question of how large the set of LR states is. The set of all graph states of N qubits consists of $2^{\binom{N}{2}}$ elements, including all possible isomorphisms and graphs which can be separated into two or more unconnected sub-graphs. We can easily generate LR states from the $(N-1)$ -qubit graphs by adding an extra qubit and connecting it to any single qubit from the previous graph. This state must be LR because the qubit that we have just added constitutes one such partitioning. There are at least $(N-1)2^{\binom{N-1}{2}}$ such states. Despite being a small fraction ($\sim N/2^{N-1}$) of all graph states, they certainly form a significant class in their own right. Moreover, there are further examples to be added into the class of LR graph states, but accurate enumeration is a combinatorial challenge. In Table I we present the number of LR states for graphs of up to 7 qubits.

Now that we have provided a lower bound, is it possible to either tighten this bound, or give an upper bound? Let us consider all possible graph states of N qubits. We shall select a specific partition of $q < N - q$ qubits. The probability, p_q , that local reconstruction is possible across this boundary is given by

$$p_q = \sum_{b=0}^q \frac{\binom{q}{b} \binom{N-q}{b} b!}{2^{q(N-q)}}.$$

This is a result of requiring that there are $q(N-q)$ possible bonds across the partition, which could either be bonded or not. Of these $2^{q(N-q)}$ combinations, only those with no more than a single bond from each qubit make the state locally reconstructible. For b bonds across the partition, we have to choose them from q on one side and $N-q$ on the other side. Finally, the ordering of the choice on one side of the partition is important, hence the $b!$. This can be expressed in terms of the confluent hypergeometric function,

$$p_q = 2^{q(q-N)} (-1 + (-1)^q U(-q, 1 - 2q + N, -1)).$$

There are $\binom{N}{q}$ ways that we could have chosen a partition of q qubits. Each of these has the same probability of giving local reconstructibility, but we must make sure we do not over count the cases where there is more than

one partitioning for the same graph state,

$$P_q = - \sum_{n=1}^{\binom{N}{q}} (-1)^n \binom{\binom{N}{q}}{n} p_q^n = 1 - (1 - p_q)^{\binom{N}{q}}.$$

Similarly, we need not be restricted to a specific q , but must avoid over-counting,

$$P = \sum_{i=1}^{\lfloor N/2 \rfloor} P_i - \sum_{j < i} P_i P_j + \dots$$

To simplify this expression, we can take the smallest (largest) value of P_q and assume that all P_q have this value, thereby lower (upper) bounding P .

$$P \geq - \sum_{n=1}^{\lfloor N/2 \rfloor} \binom{N/2}{n} (-1)^n P_{\min}^n = 1 - (1 - P_{\min})^{N/2}.$$

The bounds will occur for $q = 1$ and $q = N/2$. In the case of $q = 1$, $p_q = (N-1)/2^{N-1}$ and hence the fraction of LR states is estimated to be $N^3/2^N$. To see that this is an upper bound, we write that $p_q \sim 2^{q(q-N)} O(N^q)$ and $P \approx p_q \binom{N}{q} \frac{N}{2}$, having assumed that a particular value of q is going to give the required bound. The ratio for successive values of q is therefore given by

$$\frac{P|_q}{P|_{q-1}} = \frac{N-q}{q} \cdot O(N) \cdot 2^{2q-N-1}.$$

Hence, each successive value of P must be smaller given the overpowering nature of the exponential 2^{-N} . Therefore the bound which we have just derived is an upper bound. Combining this with our existing lower bound,

$$\frac{N-1}{2^{N-1}} \leq \frac{|LR_N|}{|G_N|} \leq \frac{N^3}{2^N}.$$

APPENDIX B: THE PERFORMANCE OF THE DIVIDE AND REBUILD PROTOCOL

In the body of the paper, we focused on calculating upper bounds for certain types of noise, and comparing them to a numerical analysis of the performance of the GMPP. We have also analyzed the DRPP in the case of local- Z noise, when we can show that it is optimal. In general, we do not expect this protocol to be optimal, but it is still useful because we can analyze its performance, and use it to place a lower bound on the performance of any optimal protocol.

1. Maximally Depolarizing Noise

We can readily show that the DRPP does not adapt well in the presence of some correlated noise (of course, X and Y -errors can be represented as correlated Z -errors, so

we have optimality in some special cases). For example, we can take the case of the maximally depolarized state of N qubits,

$$\rho_N = \frac{\mathbb{1} + x|\psi_G\rangle\langle\psi_G|}{2^N + x}.$$

and consider $|\psi_G\rangle$ to be the N -qubit linear cluster state. When we perform measurements on this state, we reduce it from $\rho_N(x) \rightarrow \rho_{N-1}(x/2) \rightarrow \rho_2(x/2^{N-2})$. The bipartite state can be purified if

$$\frac{1 + \frac{x}{2^{N-2}}}{4 + \frac{x}{2^{N-2}}} > \frac{1}{2}$$

and hence the fidelity goes as

$$\langle\psi_G|\rho|\psi_G\rangle > \frac{1}{3} + \frac{1}{3 \cdot 2^{N-1}}$$

which tends to a fixed value of $1/3$, whereas genuine multipartite purification protocols can purify states exponentially decreasing fidelities [12].

2. Local Depolarizing Noise

We would also like to demonstrate the performance of the DRPP when we do not know what the type of local error is. We proceed by assuming that the noise is the most destructive type of local noise considered here. This is simply Z -noise, because these errors form a complete basis for the state, whereas other types of error need not. Errors occur with probability p , with an equal likelihood of them being either X , Y or Z . Making a Z -measurement hence causes the propagation of an error to another qubit in $2/3$ of the cases. The simplicity of the protocol, however, continues to help us, enabling the calculation of the critical error probability, p_{crit} assuming that the graph has a maximum degree of D_G . Note that it is necessary to assume that the graph is two-colorable, which means that an error can only propagate to one of the two qubits in the Bell pair to be purified.

Consider a single Bell-pair, which is the one which we aim to measure towards and purify. Each qubit is attached to $D_G - 1$ other qubits in the graph. We will be able to purify the state if the probability of error on the Bell pair, after measurement of the other qubits, is better than $\frac{1}{2}$. The probability of an error occurring on a single qubit is p , and it is equally likely to be X , Y or Z . Let q be the probability that all the qubits attached to one of the pair give no errors on the qubit they are attached to after Z -measurements. This is caused by no errors occurring, Z errors occurring (which do not get transmitted) or pairs of X or Y errors, which cancel when transmitted

to the final qubit.

$$\begin{aligned} q &= \sum_{n=0}^{\lfloor \frac{1}{2}(D_G-1) \rfloor} \binom{D_G-1}{2n} \left(\frac{2p}{3}\right)^{2n} \\ &\times \sum_{m=0}^{D_G-1-2n} \binom{D_G-1-2n}{m} (1-p)^{D_G-1-2n-m} \left(\frac{p}{3}\right)^m \\ &= \frac{1}{2} (1 + (1 - 4p/3)^{D_G-1}) \end{aligned}$$

If $g(n)$ is the probability that n errors occur on the Bell pair due to its local errors (i.e. neglecting the connected qubits), then after measurements there is no error with a probability

$$g(0)q^2 + g(1)q(1-q) + g(2)(1-q)^2.$$

No errors occur on the Bell pair if no errors truly occurred, $(1-p)^2$, or pairs of errors cancel (YY , ZX , XZ), $p^2/3$. Hence, $g(0) = (1-p)^2 + p^2/3$. Similarly, we find that $g(2) = \frac{1}{2}g(1) = 1 - g(0)/3$. Substitution of these yields the polynomial

$$x^{2D_G} + 2x^{D_G+1} - 1 = 0$$

where $x = 1 - 4p/3$ and p is the critical error rate below which this protocol will perfectly purify the state. In the case of the Steane code, $D_G = 3$, and hence $p_{\text{crit}} = 0.16$. As stated in the body of the paper, existing multipartite purification protocols improve upon this probability.

3. Fully Connected Graph States

As an example of the application of the DRPP, we will examine the purification of fully-connected graph states. Note that these graphs are not LR, although they are locally equivalent to GHZ states, and hence have been indirectly included in previous discussions. We shall start by considering the triangular configuration of Fig. 5(c).

Given the small size of the triangle, examination of the different local error combinations is tractable. There are $3^3 = 27$ different combinations of local errors. Of these, 12 can be turned into independent local Z -noise on the 3-qubit chain using the equivalence of graphs under local unitaries. These are the combinations XXY , XYZ and ZZY and their permutations. Two further cases of particular interest are local X -noise and local Y -noise. Our protocol of measuring a single qubit (in the X -basis in this case) can tolerate an error probability of $p < \frac{1}{2}$ for X -noise. This is because pairs of errors obey identities such as $X_2X_3 = X_1$, and hence an X -measurement on qubit 1 commutes with these errors.

The ultimate realization of this is in the case of independent local Y -noise, since a Y -error is the same as correlated Z -errors on all 3 qubits. Hence, all the Y -errors are the same, and a single Y -measurement would eliminate all of them. However, a single Y -measurement leaves all the other qubits in a separable state – all the

bonds are broken, not just those connected to the qubit that is measured. Instead, we must perform some other measurement. A Z -measurement, for example, allows purification for all errors since one of the two diagonal elements is always larger than $\frac{1}{2}$.

The results derived for a triangular graph for both local X -noise and local Y -noise hold for all fully connected graphs,

$$|G_N\rangle = \frac{1}{\sqrt{2^N}} \sum_{i=0}^{2^N-1} (-1)^{\binom{w_i}{2}} |i\rangle,$$

where w_i is the binary weight of the number i . In the case of Y -noise, a single Y -error is the same as correlated Z -errors across all qubits, so all Y -errors are the same, and the noisy state only has two diagonal elements, the first of which is the probability that an even number of errors occurred,

$$\begin{aligned} f &= \sum_{n=0}^{\lfloor N/2 \rfloor} (1-p)^{N-2n} p^{2n} \binom{N}{2n} \\ &= \frac{1}{2} ((1-2p)^N + 1) \end{aligned}$$

Upon performing a Z -measurement on one of the qubits, we are left with the state $|G_{N-1}\rangle$ and the diagonal elements must be the same as they were before. This can be verified by writing

$$|G_N\rangle = \frac{1}{\sqrt{2^N}} \sum_{j=0}^{2^{N-1}-1} (|0\rangle + (-1)^{w_j} |1\rangle) (-1)^{\binom{w_j}{2}} |j\rangle. \quad (\text{B1})$$

Note that $(-1)^{w_j} |j\rangle = Z^{\otimes N} |j\rangle$ if j is an N -bit binary string, which means that if we get the $|1\rangle\langle 1|$ result, the corrective unitary is a Z -rotation on every qubit. This reduction to fully connected graphs continues to the case of $|G_2\rangle$, which we know can always be purified if it only has two diagonal elements since one element is always greater than $\frac{1}{2}$.

In the case of X -noise, we must verify that an X -measurement on a single qubit reduces $|G_N\rangle$ to $|G_{N-1}\rangle$. After applying $|+\rangle\langle +|$ to the state in Eqn. (B1), we are left with a sum over binary strings of even weight. To convert this into $|G_{N-1}\rangle$, we apply a Hadamard on one

qubit, and Z -rotations on all the other qubits. Since the independent X errors commute with this measurement process, this will eventually reduce to the triangle, which we have already solved, and hence $p < \frac{1}{2}$ is the criterion for purification. Note, however, that when reducing to a two-qubit state, our density matrix has 3 diagonal elements, not 2 as in the case of Y errors, so purification at $p > \frac{1}{2}$ is not possible with this protocol.

APPENDIX C: FIXED POINTS OF BIPARTITE PURIFICATION

In [29], a bipartite purification protocol was proposed for which subsequent analysis [30] showed that its behavior is very similar to that of the GMPP, with the added advantage that we can calculate its performance. As an example, let us consider maximally depolarizing noise applied to a linear state of N qubits. For simplicity, and consistency with [30], we shall define $D = 2^{N/2}$, assuming that there are $N/2$ qubits either side of the bipartite split. The diagonal elements of the initial density matrix, $\lambda_{kj}^{(0)}$ indicate the errors k and j either side of the partition. After n iterations of the protocol, the unnormalized outcome is

$$\lambda_{kj}^{(n)} = \sum_{k'=0}^{D-1} e^{-\frac{2\pi i k k'}{D}} \left[\sum_{k''=0}^{D-1} e^{-\frac{2\pi i k'' k'}{D}} \lambda_{k''j}^{(0)} \right]^{(2^n)}.$$

For maximally depolarizing noise,

$$\lambda_{kj}^{(0)} = \frac{1}{D^2 + x} + \delta_j \delta_k \frac{x}{D^2 + x}.$$

Following this through and renormalizing, we find that

$$\lambda_{00}^{(n)} = \frac{(x+D)^{2^n} + (D-1)x^{2^n}}{D[(x+D)^{2^n} + (D-1)D^{2^n}]}.$$

For $x = D$, $\lambda_{00}^{(n)}$ is independent of n , and hence we have found a fixed point of the protocol. The implication is that there is a critical fidelity of $1/2^{N/2}$, below which the maximum achievable fidelity is $1/2^{N/2}$, and above which complete purification is possible.

-
- [1] M. Christandl and S. Wehner, LNCS **3788**, 217 (2005).
 - [2] R. Raussendorf and H. Briegel, Phys. Rev. Lett. **86**, 5188 (2001).
 - [3] R. Raussendorf, D. E. Browne, and H. J. Briegel, Phys. Rev. A **68**, 022312 (2003).
 - [4] Y. Lim, A. Beige, and L. Kwak, Phys. Rev. Lett. **95**, 030505 (2005).
 - [5] S. D. Barrett and P. Kok, Phys. Rev. A **71**, 060310(R) (2005).
 - [6] D. Gross, K. Kieling, and J. Eisert (2006), quant-

- ph/0604217.
- [7] D. Deutsch, A. Ekert, R. Jozsa, C. Macchiavello, S. Popescu, and A. Sanpera, Phys. Rev. Lett. **77**, 2818 (1996).
- [8] C. H. Bennett, G. Brassard, S. Popescu, B. Schumacher, J. A. Smolin, and W. K. Wootters, Phys. Rev. Lett. **76**, 722 (1996).
- [9] H.-J. Briegel, W. Dür, J. I. Cirac, and P. Zoller, Phys. Rev. Lett. **81**, 5932 (1998).
- [10] M. Murao, M. B. Plenio, S. Popescu, V. Vedral, and P. L.

- Knight, Phys. Rev. A **57**, 4075(R) (1998).
- [11] W. Dür, H. Aschauer, and H.-J. Briegel, Phys. Rev. Lett. **91**, 107903 (2003).
 - [12] H. Aschauer, W. Dür, and H.-J. Briegel, Phys. Rev. A **71**, 012319 (2005).
 - [13] C. Kruszynska, A. Miyake, H. J. Briegel, and W. Dür (2006), quant-ph/0606090.
 - [14] S. Glancy, E. Knill, and H. M. Vasconcelos (2006), quant-ph/0606125.
 - [15] K. Goyal, A. McCauley, and R. Raussendorf (2006), quant-ph/0605228.
 - [16] R. Raussendorf, S. Bravyi, and J. Harrington, Phys. Rev. A **71**, 062313 (2005).
 - [17] S. L. Braunstein, C. M. Caves, R. Jozsa, N. Linden, S. Popescu, and R. Schack, Phys. Rev. Lett. **83**, 1054 (1999).
 - [18] G. Vidal and R. Tarrach, Phys. Rev. A **59**, 141 (1999).
 - [19] W. Dür and J. I. Cirac, Phys. Rev. A **61**, 042314 (2000).
 - [20] A. Kay, J. K. Pachos, W. Dür, and H.-J. Briegel, New J. Phys. **8**, 147 (2006).
 - [21] M. Hein, J. Eisert, and H. J. Briegel, Phys. Rev. A **69**, 062311 (2004).
 - [22] F. Verstraete and J. I. Cirac, Phys. Rev. A **70**, 060302(R) (2004).
 - [23] M. Hein, W. Dür, J. Eisert, R. Raussendorf, M. V. den Nest, and H.-J. Briegel, in *Proceedings of the International School of Physics “Enrico Fermi” on “Quantum Computers, Algorithms and Chaos”* (quant-ph/0602096, 2005).
 - [24] B. Zeng, H. Chung, A. W. Cross, and I. L. Chuang (2006), quant-ph/0611214.
 - [25] W. Dür and H.-J. Briegel, Phys. Rev. Lett. **92**, 180403 (2004).
 - [26] M. Horodecki, P. Horodecki, and R. Horodecki, Phys. Lett. A **223**, 1 (1996).
 - [27] A. Peres, Phys. Rev. Lett. **77**, 1413 (1996).
 - [28] F. Verstraete, J. Dehaene, and B. D. Moor, Phys. Rev. A **65**, 032308 (2002).
 - [29] G. Alber, A. Delgado, N. Gisin, and I. Jex, J. Phys. A **34**, 8821 (2001).
 - [30] M. A. Martín-Delgado and M. Navascués, Eur. Phys. J. D **27**, 169 (2003).
 - [31] F. Verstraete, M. A. Martín-Delgado, and J. I. Cirac, Phys. Rev. Lett. **92**, 087201 (2004).
 - [32] F. Verstraete, D. Porras, and J. I. Cirac, Phys. Rev. Lett. **93**, 227205 (2004).
 - [33] I. Affleck, T. Kennedy, E. H. Lieb, and H. Tasaki, Commun. Math. Phys. **115**, 477 (1988).
 - [34] W. Dür, L. Hartmann, M. Hein, M. Lewenstein, and H.-J. Briegel, Phys. Rev. Lett. **94**, 097203 (2005).
 - [35] M. Popp, F. Verstraete, M. A. Martín-Delgado, and J. I. Cirac, Phys. Rev. A **71**, 042306 (2005).